

4. EXPERIMENTAL FACILITIES IN BEAM HALL

4.1 GENERAL PURPOSE SCATTERING CHAMBER (GPSC)

M. Archunan, Golda K. S., A. Kothari, P. Barua, P. Sugathan and R.K. Bhowmik

This facility has been used for experiments in various fields of Physics viz. Nuclear Physics, Material Science, and Atomic Physics. Many attachments and alternations are made in the mechanical structure and control system of this chamber as per the unique requirement of each experiment carried out. There is provision to use the part of the existing National Array of Neutron Detectors (NAND), along with GPSC for neutron measurements in nuclear physics experiments. A couple of experiments have been carried out using this facility to study the dynamics of heavy ion induced fusion-fission reactions. The stand alone NAND facility has also been used for neutron multiplicity measurements using both Pelletron and LINAC beams.

4.1.1 Neutron Cross-talk in Modular Detector Arrays- a Monte-Carlo Simulation

Golda K.S. and R.K. Bhowmik

Neutron scattering is a matter of concern while designing the geometry of a modular detector array. The support structure under consideration for the upcoming modular neutron array at IUAC is a geodesic dome of icosahedron symmetry with frequency 4. The detectors can be arranged in such a structure at a distance of 1 metre from the target with the neighbouring detectors subtending an arc of $\sim 15^\circ$, corresponding to a distance of ~ 25 cm from each other.

A Monte-Carlo simulation to study the cross talk probability for neutrons, produced in heavy ion induced fusion-fission reaction at near barrier energy [2], has been carried out using GEANT3 [1]. Neutron transport has been simulated by GCALOR [3] and neutron cross sections adopted from MICAP [4]. Tracking of neutrons and charged particles has been done through GEANT3. Nonlinear light response curve for protons and alpha particles has been adopted from MODEFF [5]. Statistical fluctuations for light output and time resolution of the detecting system have been incorporated.

Detector efficiency and neutron scattering has been reproduced for DeMoN array [6]. Preliminary results indicate that cross talk events have longer TOF and reduced light output (average kinetic energy < 1 MeV) which enables us to separate cross talk events to a greater extend by putting a threshold in the light out put. It is important to notice that the ratio of crosstalk to true n-n coincidence rate in the present geometry is insensitive to flight path and detector dimensions and strongly depends on the angular separation between the neighboring detectors. The calculations show that cross talk can be minimized in coincidence data by suppressing only the nearest neighbor events. Further reduction of cross talk is possible by

incorporating a TOF dependent light threshold. For the proposed geometry, the cross talk contribution in singles due to scattering from a neighbouring detector is $\sim 0.2\%$ (fig 1).

REFERENCES

- [1] <http://wwwasd.web.cern.ch/wwwasd/geant/index.html>.
- [2] K. S. Golda, and R. K. Bhowmik, DAE Symp. Nucl. Phys. 54, 658 (2009).
- [3] <http://www.staff.uni-mainz.de/zeitnitz/Gcalor/gcalor.html>.
- [4] <http://www-rsicc.ornl.gov/codes/psr/psr2/psr-261.html>.
- [5] R. A. Cecil, B. D. Anderson, and R. Madey, Nucl. Instrum. Methods 161, 439 (1979).
- [6] I. Tilquin, et.al., Nucl. Instr. and Meth. A 365 (1995) 446.

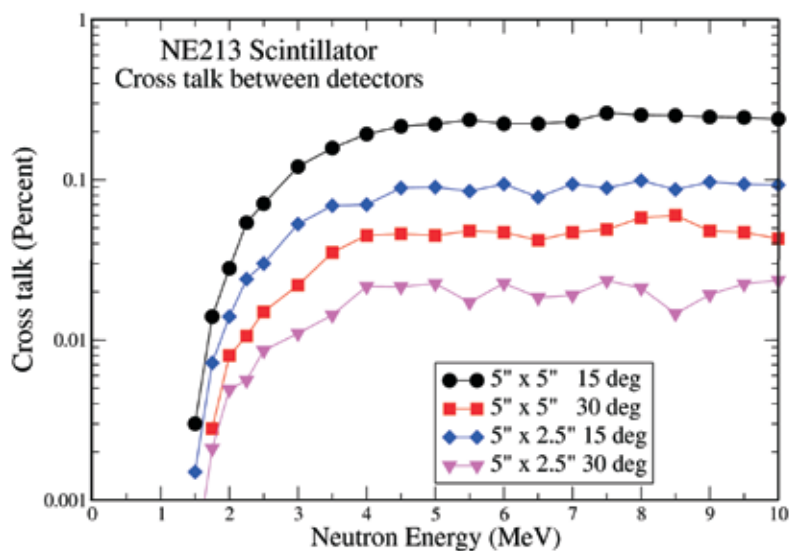


Fig. 1. Neutron cross talk as a function of energy

4.2 GAMMA DETECTOR ARRAY (GDA)

Kusum Rani, S.K. Saini, A. J. Malyadri, Rajesh Kumar, S.K. Suman, Archunan, Ashok Kothari, P. Barua, E.T. Subramaniam, Mamta Jain, S. Venkataramanan, Arti Gupta, S. Rao, U. G. Naik, Raj Kumar, S. Muralithar, R.P. Singh, Rakesh Kumar, N. Madhavan, S. Nath, J. Gehlot, J.J. Das, P. Sugathan, A. Jhingan, T. Varughese, K.S. Golda, D. Negi, Anukul Dal, Gellanki Jnaneswari, Tarkeshwar Trivedi, Kumar raja and R. K. Bhowmik

The users of INGA and GDA facilities have published prolifically this year contributing over 34 contributions in DAE 2009 and 13 communications in international journals. The

primary activity in this year was devoted in experiments using the INGA facility in Beam Hall II.

4.2.1 Indian National Gamma Array (INGA)

The Indian National Gamma Array (INGA) was installed in beam hall II at IUAC in January, 2008 and a series of experiments were carried out [1]. The Data Acquisition System (DAS - Candle) was upgraded recently with multi-crate system consisting of three CAMAC crates. Using this DAS, multi fold coincidence data were collected from INGA. Apart from coincidence data, scaled singles data from radioactive sources were also collected for each experiment.

One of the important requirements for establishing the level scheme of a nucleus is to extract the relative angular distributions of the levels populated in the reaction. Typically such an analysis is done using an average efficiency curve for a representative detector in the array. The present exercise is an attempt to show that it is important to take into account the variation in the efficiency curves for individual detectors for a reliable extraction of angular correlation. In order to calibrate the array with respect to data correlation between different detector combinations, the measurement of angular correlation of ^{60}Co γ -rays using INGA array was taken up.

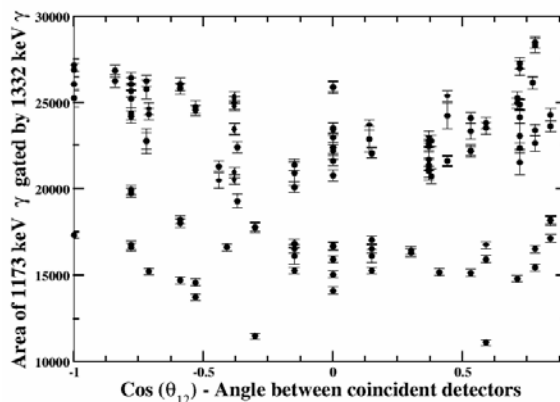


Fig. 1. Total counts for 1173 keV \times 1332 keV coincidences between different pairs of detectors as a function of θ_{12}

At the time of measurement, eleven Compton suppressed clover Germanium detectors were available. The data were taken both in pre-scaled singles and in doubles mode using ^{152}Eu and ^{60}Co sources. The area under 1173 keV peak in coincidence with 1332 keV for different detector combinations are plotted in Fig 1 as a function of relative angle θ_{12} between the detectors.

Careful analysis of singles data showed that although different detectors are expected to have similar efficiency at different energies, actual measurements indicated large variations

both in lower and higher energies as shown in Fig 2. It's to be noted that all detectors are mounted at nominally same distance of 24 cm from the source and all four crystals of these detectors are used in add-back mode. The counting rates in photo-peak at lower energies are also dependent on the absorbers (the target holding rods) coming in front of some detectors. The counting rate varies by as much as 12 % depending on the shadow of source holder on detector.

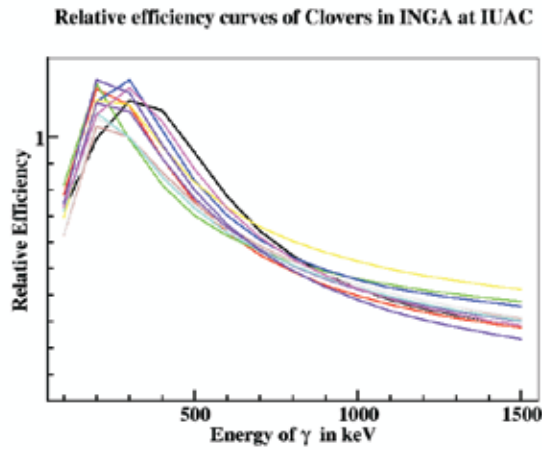


Fig 2. Variation of efficiency curves for different detectors in INGA array

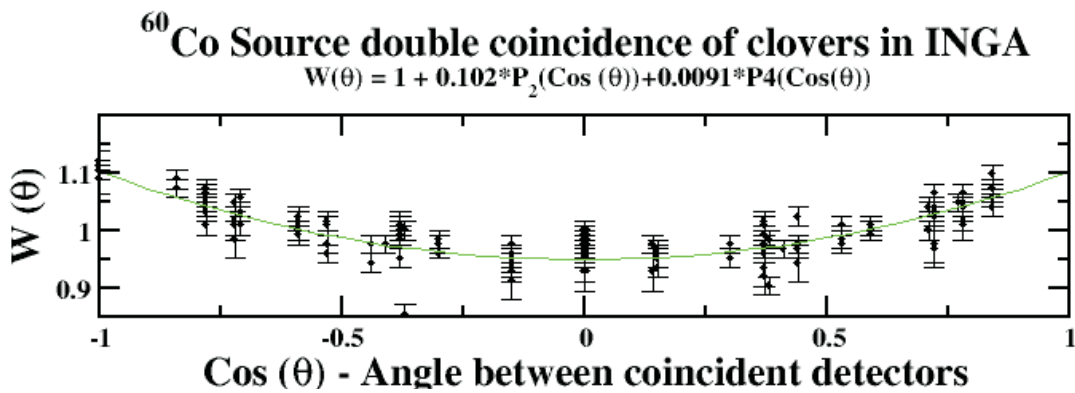


Fig 3. Normalized angular correlation between different pairs of detectors

After individual detector efficiency corrections, the normalized coincidence data follows the trend as expected from theory[2] which is shown as solid curve (Fig 3). This study shows that it is possible to reliably extract the relative angular distribution of various transitions from INGA data provided the respective detectors efficiency are taken into account. This also confirms that the data coming from the three CAMAC crates are treated on equal footing by the data acquisition hardware [3], data collection software CANDLE[4] and the offline analysis code INGASORT.

Polarization sensitivity of Clover detector was used to measure the linear polarization of γ -rays from the reaction $^{94}\text{Mo}(^{16}\text{O},\text{xnp})$ reaction at beam energy of 70 MeV. The data were collected in γ - γ coincidence mode. The geometrical factor was measured for Clover detectors using a ^{152}Eu source in singles mode. It was measured on an average to be 0.98(2). Fig.4 shows the γ -ray coincidence spectrum of normalized Compton scattered events in perpendicular plane and parallel coincidence events from 90° Clover detector. γ transition of ^{106}Cd [5] has more coincidences in perpendicular scattering than in parallel scattering. It is vice versa for magnetic dipole type 612 keV transition in ^{107}In [6] and the magnetic quadrupole type 641 keV of ^{107}Cd [7].

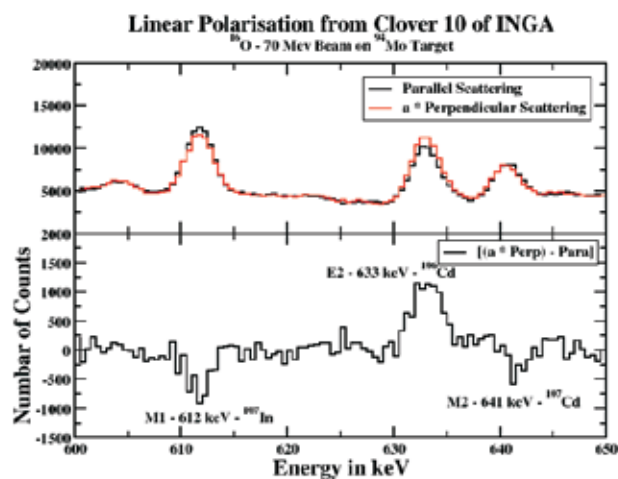


Fig. 4. Polarization sensitivity of clover detector (see text)

REFERENCES

- [1] S. Muralithar, et. al., DAE-BRNS Symp. on Nucl. Phys., Vol 53(2008)689, Vol 52(2007)595.
- [2] K.Siegbahn, Ed., Alpha-Beta- and Gamma-Ray spectroscopy, North Holland Publishing Co., Amsterdam (1965).
- [3] Kusum Rani, Annual report of IUAC (2002-2003)43.
- [4] Ajith Kumar B.P., et. al. DAE-BRNS Symp. on Nucl. Phys., Vol. 44B(2001)390.
- [5] P. Regan et. al., Nucl. Phys. A 586 (1995) 351.
- [6] D. Negi et. al., to be communicated.
- [7] D.C. Stromswold et. al., Phys. Rev. C 17 (1978) 143.

4.2.2 Experiments using GDA / INGA related facilities

The INGA was used in this year by various users. The phenomena which were addressed by experiments were Chirality, Magnetic Rotational band, incomplete fusion, study of collectivity, isospin symmetry breaking, Superdeformed bands, and Terminating bands. There were in total eighteen experiments conducted using this facility (refer table).

<i>Date</i>	<i>Description</i>	<i>User</i>
27-5-09	<i>Spectroscopy and lifetime measurements in La and Pr (A=135) Nuclei</i>	<i>Ritika Garg Delhi University</i>
4-6-09	<i>High spin structure and DSAM measurements in ^{131,132}Ba</i>	<i>Ashok Kumar Punjab University</i>
8-6-09	<i>Study of absorptive break-up (incomplete fusion) dynamics in heavy-ion interaction at E/A ~ 4-7MeV</i>	<i>Rakesh Kumar IUAC</i>
12-6-09	<i>The question of dynamic chirality in nuclei: The case of ¹⁰²Rh</i>	<i>D. Tonev LNL-INFN, Italy</i>
19-6-09	<i>Search for Terminating Bands in A=110 Mass region, ¹¹¹, ¹¹²Sn, ¹¹³Sb</i>	<i>P. Bannerjee SINP, Kolkata</i>
27-6-09	<i>Structure of bands in ^{125,127}I</i>	<i>H.P. Sharma BHU, Varanasi</i>
8-7-09	<i>Single particle states in heavy nuclei intruder proton level structure above Z=82 in ^{194,195}Bi</i>	<i>Gopal Mukherjee VECC, Kolkata</i>
15-7-09	<i>Spectroscopy of ¹²⁶I using compound nuclear reaction</i>	<i>Pragya Das IIT, Mumbai</i>
25-7-09	<i>Search for chiral partner bands in ⁹⁸Tc</i>	<i>Rishi Kr. Sinha BHU, Varanasi</i>
4-8-09	<i>Search of new coupling schemes in the A=110 and 135 mass regions</i>	<i>Deepika Choudhuri IIT, Roorkee</i>
16-8-09	<i>Wobbling and multi-quasiparticle bands in ^{168,169}Re isotopes</i>	<i>Gautam Ganguly Calcutta University</i>
26-8-09	<i>Transition rates in mirror nuclei ³⁵Ar and ³⁵Cl- a test of isospin symmetry breaking</i>	<i>Maitreyee Sarkar SINP, Kolkata</i>
3-9-09	<i>Triaxial Bands in ¹³⁹Pr</i>	<i>Somen Chanda Calcutta University</i>
11-9-09	<i>Study of structure of nuclei near A=120 – ^{121, 122}La, ¹¹⁹Ba, ¹¹⁹Cs</i>	<i>U. Datta Pramanik SINP, Kolkata</i>
19-9-09	<i>Feeding and decay of the superdeformed band in ¹³³Nd</i>	<i>I. Majumdar TIFR, Mumbai</i>
10-10-09	<i>Study of Hyperfine interactions by PAD technique</i>	<i>A.K Bhati Punjab University</i>
6-11-09	<i>RDD Facility Test in INGA</i>	<i>RP Singh IUAC</i>
4-2-10	<i>Probing of Reaction Dynamics Using Light-Heavy Ion Beams</i>	<i>B. P. Singh A. M. University</i>

4.3 RECOIL MASS SPECTROMETERS

4.3.1 Heavy Ion Reaction Analyzer (HIRA)

N. Madhavan, S. Nath, J. Gehlot, T. Varughese, A. Jhingan, P. Sugathan, GDA Group, S. Kalkal¹, S. Mandal¹, R. Singh¹, E. Prasad², G. Mohanto

¹Department of Physics and Astrophysics, Delhi University, Delhi

²Department of Physics, Calicut University, Calicut, Kerala

The excellent primary beam rejection, large transmission efficiency and mass resolution of HIRA were put to use in transfer measurements around barrier. Electrostatic dipoles ED1 and ED2 of HIRA had to be operated at high fields due to the large kinetic energy of target-like recoils selected by HIRA, which required additional high voltage conditioning.

HIRA was used to study the effect of transfer channel coupling on the sub-barrier fusion cross section enhancement in the systems $^{28}\text{Si} + ^{90,94}\text{Zr}$ by detecting the transfer channels using kinematic coincidence method. Earlier, fusion excitation function down to well below barrier, evaporation residue (ER) transmission efficiency and angular distribution of ERs had been studied using HIRA as reported in last year's annual report. For the $^{28}\text{Si} + ^{90}\text{Zr}$ system, the enhancement could be explained only by coupling inelastic excitation channels. A substantial increase in sub-barrier fusion cross-section was observed for the latter system beyond the predictions of coupled channels calculations that included prominent inelastic excitations both in projectile and target. The system $^{28}\text{Si} + ^{90}\text{Zr}$ has Q-value transfer channels all negative, while $^{28}\text{Si} + ^{94}\text{Zr}$ has positive Q-value transfer channels up to 4n-pickup channel. This makes the measurement of transfer channels interesting and relevant.

Transfer reaction around and below barrier is peaked at back-angles and hence difficult to measure, especially below barrier when it peaks around 180° with respect to beam direction. HIRA, due its excellent primary beam rejection and large efficiency for such high energy target-like recoiling particles, was used in these measurements. In order to select only transfer channels, kinematic coincidence method was employed with back-scattered particles, around 165 degrees, detected in a 20mm x 20mm two-dimensional, position sensitive silicon detector; the forward moving target-like recoils were selected by HIRA and mass analyzed at the focal plane with two-dimensional, position-sensitive, large MWPC detector. The mass and energy loss of the recoils, energy of back-scattered ions, and the time-of-flight (TOF) difference between the two set of particles were recorded event-by-event. Detailed simulation and experimental checks were done to ensure the same coincidence efficiency for elastic scattering and transfer channels. The elastic channel was then used to normalize the various transfer channels

which gives an in-built normalization procedure. A thin carbon (charge state reset foil) placed nearly 10 cm downstream of target helped in proper charge state setting of HIRA and in realizing its theoretical transmission efficiency.

The energy spectra of the back scattered particles, gated by individual masses of recoiling particles at focal plane, were used to extract the Q-value spectra of the various transfer channels using the energy calibration. Coincident condition and time-of-flight (using pulsed beam) were used to reject any beam-like particle condition at the focal plane. Fig. 1 shows the schematic of the coincidence measurement setup and Fig. 2 the mass spectra of the particles detected at HIRA focal plane.

Two sets of BGO detectors (7 each, above and below the target at a distance of 4 cm from the target) were used to select the gamma rays in coincidence with focal plane events. This gives a measure of the relative yield of transfer to excited states and to the ground state.



Fig.1. Kinematic coincidence setup showing the mean angles for projectile-like and target-like particles

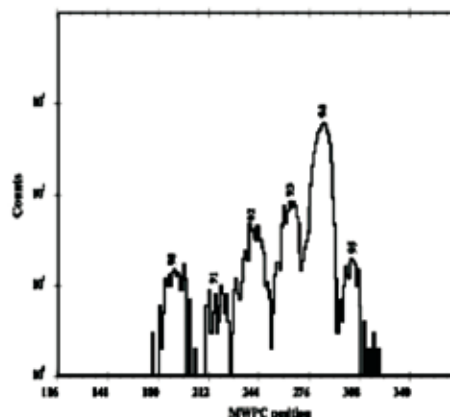


Fig.2. Mass spectrum for the central charge state in $^{28}\text{Si} + ^{94}\text{Zr}$ at lab energy of 94 MeV

One important point in selecting genuine transfer events is the correction required for presence of trace target impurities in the enriched target. Detailed measurements were carried out at a laboratory energy of 70 MeV (much below the nominal Coulomb barrier) to select the other mass impurities and to quantify them relative to elastic event from predominant target nucleus. As transfer cross-section is expected to be negligible at 25% below the barrier, this is an effective method for impurity checks in target. The correction factors were used to get the actual transfer events.

The focal plane mass spectrum versus the time-of-flight for $^{28}\text{Si} + ^{90}\text{Zr}$ elastic and transfer events is shown in Fig. 3 and that for $^{28}\text{Si} + ^{94}\text{Zr}$ is shown in Fig. 4 for beam energies just above the barrier. The time-of-flight is used to resolve the m/q ambiguity, which causes

more than one mass group but with same m/q value to arrive at the same position at the focal plane. The Q -value arguments were used to assign neutron or proton transfer to the selected events. As expected, the one nucleon stripping channel is due to proton stripping from the projectile and the pick-up channels were found to be neutron pick-up by the projectile.

In $^{28}\text{Si} + ^{94}\text{Zr}$ case, transfer up to 4 neutron pick-up and 1 proton stripping could be clearly seen, separated well from each other and the elastic channel. Two nucleon transfer was pronounced in both the cases and transfer to excited and ground states were comparable in strength. The comparison of these two systems with additional gamma tagging can throw light on relative strengths of successive and sequential transfers. Detailed analysis of the data is nearing completion.

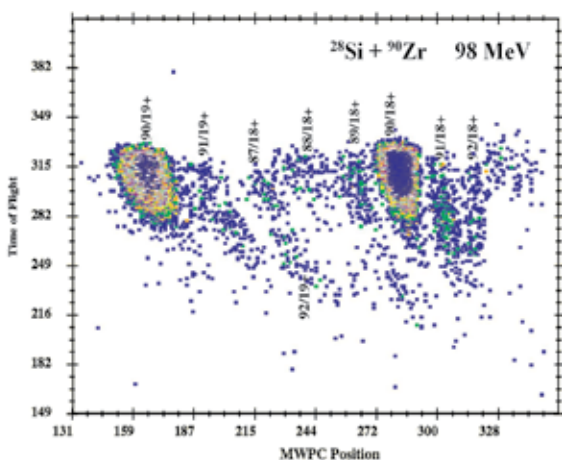


Fig. 3. M/q versus TOF for $^{28}\text{Si} + ^{90}\text{Zr}$ at lab energy of 98 MeV

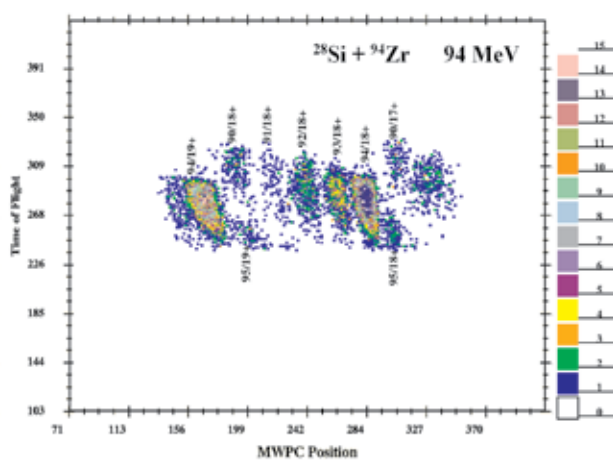


Fig. 4. M/q versus TOF for $^{28}\text{Si} + ^{94}\text{Zr}$ at lab energy of 94 MeV

4.3.2 HYBRID Recoil mass Analyzer (HYRA)

N. Madhavan, S. Nath, T. Varughese, J. Gehlot, A. Jhingan, P. Sugathan, A. K. Sinha¹, R. Singh², K. M. Varier³, M. C. Radhakrishna⁴, E. Prasad³, S. Kalkal², G Mohanto, J. J. Das, Rakesh Kumar, R. P. Singh, S. Muralithar, R. K. Bhowmik, A. Roy, P. Barua, Archunan, U. G. Naik, A. J. Malyadri, Cryogenics group, Beam transport group

¹IUC-DAE Consortium for Scientific Research, Kolkata Centre, Kolkata

²Department of Physics and Astrophysics, University of Delhi, Delhi

³Department of Physics, Calicut University, Kerala

⁴Department of Physics, Bangalore University, Bangalore

HYRA has been used in gas-filled mode to select heavy evaporation residues (ERs) in an experiment and to select heavy target-like recoils in a test run. The primary beam rejection in both the cases has been excellent as described later. The transmission efficiency for ERs has been extracted with modified entrance window foil position. Earlier, we had reported the difficulty in extracting the transmission efficiency by coincident gamma method due to intense singles gamma rays from the thick entrance window foil located close to the target. We have subsequently made arrangements to move the entrance window foil 30 cm upstream so that the HPGe detector can be shielded from gamma rays emanating from window foil. The ratio of the number of ER gated gamma ray of particular energy to the corresponding number in singles spectrum gave the transmission efficiency of HYRA in the present run. To take care of additional angular straggling effects when window foil was moved upstream, the transmission efficiency with the same electromagnetic setting was scaled by the ratios of (ER count rates/ Monitor counts) in both the runs. An efficiency of 2.6 % for ERs was extracted in the $^{16}\text{O} + ^{184}\text{W}$ fusion-evaporation reaction at 100 MeV for a focal plane MWPC area of 57 mm x 57 mm. This is comparable to the transmission efficiency measured by Dubna group for similar kinematics with a detector area of 120 mm x 40 mm. The ER detection efficiency scales by the area of MWPC and SB (50 mm x 50 mm) detectors, which is almost 1.3 times more in the former case. There is a plan to increase the focal plane MWPC size to nearly 100 mm x 50 mm and to use two SB detectors mounted adjacent to each other, in order to increase the detection efficiency.

During the long stability tests with the first module of superconducting LINAC accelerator, we could test the efficiency of HYRA gas-filled mode to select heavy, target-like recoils in the beam direction. This task is impossible for any vacuum mode magnetic separator and is extremely difficult for vacuum mode recoil mass spectrometers such as HIRA at IUAC. However, the gas-filled mode is ideally suited for this purpose. ^{48}Ti beam of 213 MeV with 2 microsecond pulse separation was used to bombard a natural lead target and the gas-filled mode parameters (gas pressure and magnetic field settings) were optimized to select the energetic, forward moving, target-like recoils. In order to get a measure of primary beam rejection, the lead target was later replaced with aluminum target and data collected for same period of time. Fig. 1 and Fig.2 show the two dimensional spectra (energy in silicon detector

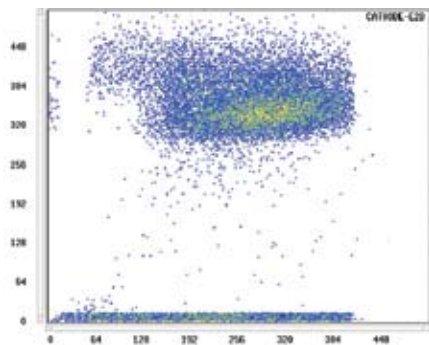


Fig. 1. Energy versus energy loss for lead-like recoils selected from ^{48}Ti + natural Pb at 0° with respect to beam

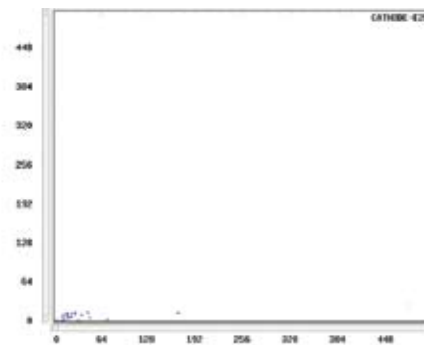


Fig. 2. Similar spectrum as Fig. 1 but with Al target (excellent beam rejection observed)

on x-axis versus energy loss in MWPC on y-axis) for natural lead target and aluminum target, respectively. The cleanliness at the focal plane and high selectivity of target-like recoils are evident from these figures. A primary beam rejection factor of better than 10^{13} was achieved.

The correlation between total energy and time-of-flight for lead-like recoils selected at the focal plane is shown in fig 3. Such a mode of operation is highly useful to populate nuclei away from the line of stability through transfer reactions around Coulomb barrier. In order to check the transmission efficiency variation, if any, with beam energy, the focal plane counts were normalized using monitor detector counts and beam energy was reduced by 15 % to get another set of data. The ratio of Rutherford scattering at two different angles, remained constant thereby showing the reproducibility of transmission efficiency when the electromagnetic fields were scaled to the new recoil energy and charge state.

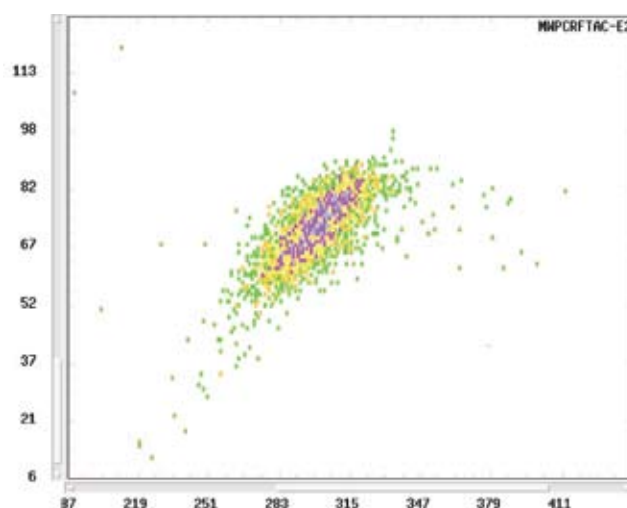


Fig. 3. Total energy (x-axis) versus measure of time-of-flight (with focal plane MWPC signal as start and RF used for pulsed beam as stop) selecting the correlated set of target-like recoiling particles

The electrostatic dipole (ED) of second stage of HYRA has been fabricated and tested for high voltage, vacuum and mechanical/alignment tolerances at M/s. Danfysik, Denmark. HYRA ED has electrodes made of solid titanium and has been tested for maximum voltages (± 300 kV across a gap of 12 cm) and at 85% field value (± 255 kV) for 8 hours with no breakdown. The high voltage tests were carried out in a current-controlled mode with 100 micro-amperes of maximum current on cathode and 120 micro-amperes of maximum current on anode and at a vacuum of about 1.0×10^{-7} Torr. The high voltage tests were carried out from outside the shielding enclosure with adequate protection from radiation and high voltage, with periodic measurements of humidity and temperature. The entire vacuum chamber and feed-thru insulators were leak checked with helium leak detector and found to have leak rate of less than 2.0×10^{-9} Torr.l/s. The top lid of ED chamber is provided with dual seal (inside metal seal and outside o-ring

seal with intermediate space roughed out) and is designed to achieve low 10^{-8} Torr when pumped with a large cryo pump. The electrodes and alignment mechanism have also been checked with jigs made for such purposes and found to match within allowed tolerances. The high voltage power supplies are suspended from the top with protective Faraday cage around and in between them, similar to HIRA EDs, to have access to floor space and for safety reasons. The high voltage feed-thru insulators can be filled with SF₆ insulating gas for better voltage handling capability at the triple junction of high voltage cable, metal and insulator.



Fig. 4. (left) ED Chamber and cryo pump (right) HV supply and Faraday cage



Fig. 5. (left) Electrode system (right) Backplane of electrode with support



Fig. 6. (left top) HV feed-thru insulator (left bottom) Anode curvature test jig (right) Alignment jig for electrode assembly

The ED chamber assembly and cryo-pumping system, power supply mounts/Faraday cage, electrode assembly and the support insulator to electrode interface, HV feed-thru insulator, anode curvature measurement jig and alignment jig are shown in figs 5-6. The successfully completed electrostatic dipole of HYRA has arrived at IUAC in dismantled and individually packed condition and the whole process of carefully assembling and aligning them, this time around by IUAC personnel, will be taken up during the second half of 2010, after a few experiments using gas-filled mode.

A two-day workshop on “Physics with HYRA” was held on May 29 and 30, 2009 at IUAC. Nearly 35 outstation participants, 15 students and several IUAC staff attended the workshop. There were 11 experimental proposals, mostly from young faculty members from universities and institutes, out of which 10 were presented and discussed at length. In the subsequent July AUC meeting, the updated proposals were presented again and have been sanctioned beam time. Four experiments propose to study fusion cross-section, three for focal plane isomer decay and one each for exclusive GDR, 180° quasi-elastic scattering and pairing/clustering effect, the last using vacuum momentum achromat mode of first stage. Next set of HYRA experiments using gas-filled mode and facility test of momentum achromat mode with beam are planned to begin soon. Experiments using full HYRA in vacuum, mass-dispersive mode and those requiring HYRA and INGA combination will be considered in future workshops.

In the near future, we plan to couple the TIFR 4π spin spectrometer (32-element NaI detector array) to HYRA first stage in order to carry out ER tagged spin distribution measurements in heavy compound nucleus formation to understand fusion-fission mechanism

in a better manner. Fig.7 shows the schematic diagram of the combination. Fig. 8 shows the alignment/support structure fabricated at IUAC to fit in the foot-print of present HYRA target chamber with provisions to open the 4π array sideways, height/tilt adjustments and mounting of electronics bins.

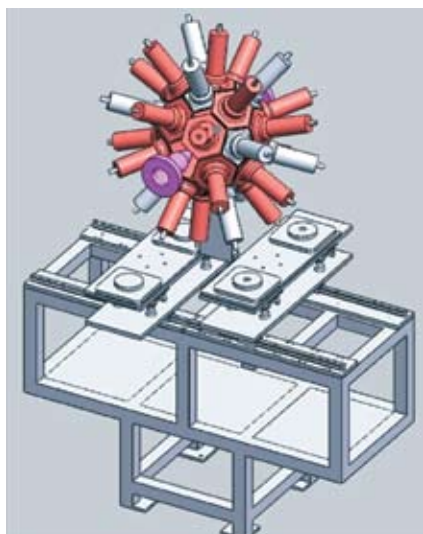


Fig.7. Schematic drawing of HYRA and TIFR 4π spin spectrometer coupling



Fig.8. Alignment/mounting structure fabricated at IUAC

INGA will be coupled to HYRA when the clover detectors arrive at the centre after TIFR campaign to realize the powerful combination of Heavy Ion Mass Analyzer coupled to Large gamma ArraY (HIMALAY) for ER tagged high spin spectroscopy.

The section of HYRA-INGA beamline for spin spectrometer and HYRA coupling uses a telescopic section for allowing more access to the spin spectrometer and the existing small aluminium target chamber used in coincidence gamma measurements. This section has been designed (Fig.9), fabricated and the telescopic section successfully vacuum tested recently.

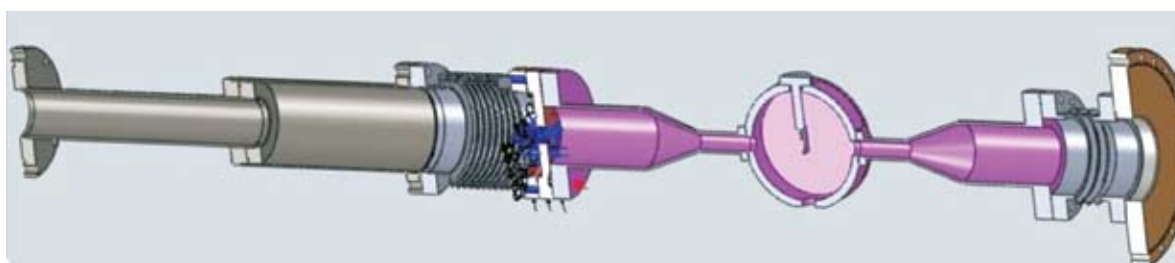


Fig. 9. Telescopic beam line section and target chamber

4.4 MATERIALS SCIENCE BEAMLIN

A. Tripathi, Ravi Kumar, K. Asokan, V.V. Sivakumar, Fouran Singh, S.A. Khan, P. K. Kulriya, I. Sulania, P. Barua, A. Kothari and D.K. Avasthi

There have been a large number of experiments in materials science with energetic ion beams. The facilities continue to support the research programmes of a large number of users from different universities and institutions from India and abroad. A total of nearly 90 user experiments comprising 250 shifts were performed this year, without any beam time loss due to major facility break down. The swift heavy ion (SHI) irradiation and related experiments are performed in the two irradiation chambers in the two materials science beamlines in beamhall I and beamhall II, and in general purpose scattering chamber (GPSC) in beamhall I. The experiments using on-line/in-situ facilities in materials science beam lines, which have unique features, were given emphasis this year. There were three on-line ERDA, three in-situ XRD, two on-line QMA and three ionoluminescence experiments. Besides that many experiments were carried out using low energy ion beams using LEIBF facility and atom beams using atom beam sputtering set up. The off-line facilities are also being used by many users for preparing and characterizing samples. Experiments are being done in different areas of SHI induced materials modification and characterization and the details of the research programmes are given in Section 5.2.

XRD, FTIR, PL, UV-Vis SPM, micro-Raman and transport measurement facilities continue to be used by a large number of users. The materials synthesis techniques: RF sputtering system, ball milling system, box furnace and tubular furnaces are being extensively used by users for preparing samples. The microwave plasma based deposition system has become operational and the installation of in-situ micro-Raman set up in the beam line is in progress.

4.4.1 Irradiation chamber maintenance

A. Tripathi, B.B. Chaudhary, S. Rao, J. Zacharias

The irradiation chamber in materials science beamline is used in most of the irradiation experiments and ERD studies. The new O-ring obtained from Huntington for the irradiation chamber didn't solve the problem being faced and a new arrangement for mounting O-rings was made for the irradiation chamber. A new aluminum ring was designed and fabricated for the new O-ring mounting arrangement as shown in Fig. 1. As the height of the chamber lid got altered with the new arrangement the sample ladder heights for the two sample ladders were adjusted and the secondary electron suppressor height was accordingly adjusted.



Fig. 1. Irradiation chamber with new o-ring system

Both the sample ladders were tested for vacuum leaks and it was found that the older sample ladder had developed a leak. A special arrangement for leak testing of the ladder was made and the leak problem was rectified by changing the central part of the sample ladder. To ensure a smooth running of the system, a spare turbomolecular pump for irradiation chamber has been acquired. New preamplifiers have also been procured for ERD facility to replace the preamplifiers that had gone bad.

4.4.2 Scanning Probe Microscope

A. Tripathi, I. Sulania

Multi Mode SPM with Nanoscope IIIa controller acquired from Digital/Veeco Instruments Inc. was extensively used in user experiments. The regular calibration and performance testing in AFM/MFM mode using standard grid and magnetic tape was conducted. This year more than 600 samples have been studied in AFM/MFM/STM (525/70/5) mode.

The SPM laboratory was re-arranged after acquisition of SEM. During re-installation of the SPM system, some problems were noticed in the software. The problem was solved with help of the company engineer. However, it was felt that the old software, which was based on Windows NT, needed upgradation and hence the software was upgraded to newer Windows XP based version. The new software was integrated to the existing controller and hardware and the system is functioning properly now. The SPM is mainly used for ion induced nanostructuring, modification of nanoparticles and other surface characterization studies.

4.4.3 In-situ X-ray Diffractometer setup

P. K. Kulriya

The Bruker D8 advance *insitu* X-ray diffractometer setup has been used extensively for offline characterization of materials in the nanoparticle, thin films as well as for the powder form. Three *insitu* experiments were performed this year. The diffractometer was used to record the diffraction pattern of the more than 850 samples from nearly 118 users from various universities/institutes this year. The total number of samples characterized using XRD setup in glancing angle and Bragg -Brentano geometry are 600 and 250 respectively. The system operation throughout the year has been smooth except for a few minor problems. There was a problem in the shutter of the X-ray tube which was traced to a malfunctioning microswitch inside the tube assembly which was replaced with new one. The water flow sensor was also found to be damaged and was replaced with a new one.

4.4.4 CCR system for in-situ XRD

P. K. Kulriya, M. Bharadwaj, R. Ahuja and D.K. Avasthi

It is desirable to perform low temperature ion irradiation and XRD measurements simultaneously in many measurements, including phase transformation studies. In view of this requirement; a GM based cryostat is procured from the “Advanced Research System” to achieve low temperature around 10K. The offline testing of the cryostat has been done and the measured minimum temperature reached is about 9.4K. The design of the low temperate cooling unit is finalized. A linear motion actuator has been ordered to move the cryostat in forward and backward direction. The cryostat will be installed to the existing diffractometer facility soon. It is funded by nano mission project of DST, New Delhi.

4.4.5 Plasma based systems for thin film deposition

V.V. Siva Kumar

For plasma based synthesis of thin films, a rf sputtering system is available and a



Fig. 2. Microwave plasma system for thin film deposition

microwave plasma system is developed. The rf sputtering system is being used for thin film depositions while the microwave plasma system is being used for studying thin film deposition by CVD/sputtering.

The rf sputtering system was operational for thin film deposition. Thin films of BCN, BaSrO₃, ZnO, ZnS and SBN were prepared. The rf sputtering system was upgraded by incorporating a Turbo Pump/Dry pump for deposition of thin films in clean vacuum. A process is developed to deposit thin films at lower pressures. In this process, initially the plasma is produced at a higher pressure (plasma striking pressure). After that, the gas flow rates and a throttle valve are used in combination to set stable deposition pressures accurately from 4 mtorr onwards, while pumping the deposition chamber using the Turbo pump/ Dry pump.

4.4.6 Field emission scanning electron microscope (FE-SEM)

A. Tripathi, D.K. Avasthi

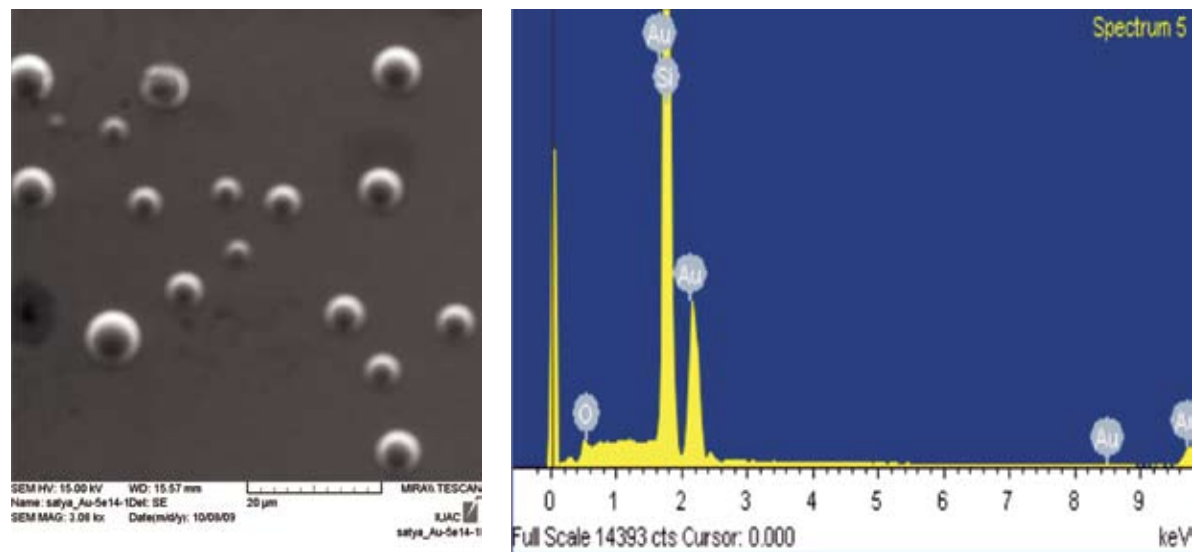
A field emission scanning electron microscope (FE-SEM) from TESCAN, MIRA II LMH CS has been installed (shown in Fig 3) to boost research activities in nanomaterials, in a project funded under Nano Initiative program of Department of Science and Technology. The SEM has a high brightness Schottky emitter electron gun with accelerating voltage variable from 200 V to 3 kV. It has a resolution of 1.5 nm at 30 kV and a 5 axis compucentric fully motorized sample stage. The system has pneumatic suspension for vibration isolation.



Fig.3. Tescan MIRA II LMH CS FE-SEM with Oxford INCA PentaFETx3 EDS

The FE-SEM system has a secondary electron detector and a backscattered electron detector for imaging. The system has five electron optics working modes in High Vacuum: (i) Resolution mode which automatically configures the column to produce the highest resolution, (ii) Depth mode which sets the column for enhanced depth of focus, (iii) Field mode which

optimizes the column to provide an extra large non-distorted field of view, (iv) Wide Field mode to provides a extra low magnification imaging with possibility of measurement and (v) Rocking Beam mode for assessment of crystal orientation data of the specimen with electron channeling pattern (ECP). The offline analysis system ATLAS has also been installed.



(a) (b)
Fig. 4. Spherical Au microballs on Si substrate: (a) SEM image with (b) EDS spectrum

The system also has an attachment for energy dispersive X ray spectrometer from OXFORD (INCA PentaFETx3) with 133 eV resolution for elemental analysis. The images of Au microballs formed on the surface of Si after irradiation and the typical EDS spectra are shown.

4.4.7 In-situ Micro-Raman facility in beam Hall II

Fouran Singh, Indra Sulania, S. K. Saini, S. Rao, B.B. Chaudhury, A. Kothari, P. Barua and D. K. Avasthi

Micro-Raman is a very efficient technique for characterization of the materials modified by swift heavy ion (SHI) irradiations. The in-situ Raman facility will facilitate systematic studies on SHIs irradiation induced modifications. It would be of particular interest to the materials which are reactive to air like semiconductors, as the surface of semiconductors get drastically modified on exposure to ambient after the SHI irradiations. Facility is equipped with Renishaw InVia Raman microscope and 50 mW Argon ion laser with 514 nm excitation. The spectrometer can scan from 100 to 3200 cm^{-1} with a very good sensitivity. An in-house designed and fabricated vacuum chamber is installed (shown in Fig

5) and aligned in the materials science beam line in beam hall II. Indigenously designed cheap and eco-friendly hydraulic lift is commissioned for lifting the lid of chamber along with x-y-z stage and target ladder. Proto-type target ladder and x-y-z fiber optic probe mount is designed, fabricated in the workshop and installed on the chamber. The system is shown in the figure below:

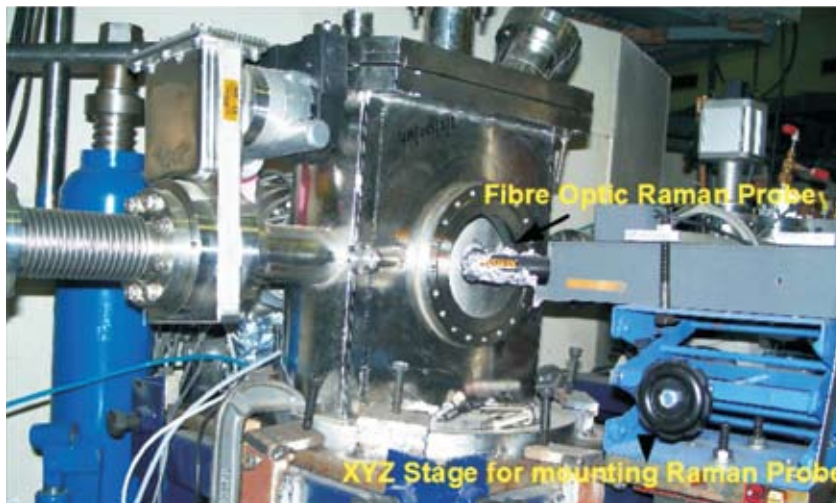


Fig. 5. In-situ Raman vacuum chamber along with accessories like fiber optic probe on x-y-z mount

The fiber optic probe was installed and tested successfully with standard samples like Si and carbon nano tubes (CNTs). Micro-Raman setup can be easily switched from in-situ to ex-situ study mode and vice versa in a few minutes. The focal length of the existing fiber optic probe is small and hence a large focal length lens assembly has been ordered to be integrated with the set up. The liquid Nitrogen (LN₂) cooled sample ladder has also been designed and the fabrication work will start shortly in the workshop.

4.4.8 Growth of Gold Nanostructures on Ion Sputtered Rippled Silica Templates

Saif A. Khan¹, D. K. Avasthi¹, K.H. Heinig², D. C. Agarwal¹ and U. B. Singh¹

¹Inter University Accelerator Centre, Aruna Asaf Ali Marg, New Delhi

²Forschungszentrum Dresden-Rossendorf, PO.Box 510119, 01314 Dresden, Germany

Several methods have been devised to create nanostructures for electronic, photonics and sensor applications. We have initiated a research program on synthesis of metal nanoparticles on silica substrates for plasmonic applications which relies on creation of rippled silica templates. For this purpose, we have prepared rippled templates of silica, as shown in Fig 1(a), by 1.5 keV Ar atom beam incident at an angle of 55° from the surface normal. Later these templates will be used to produce patterned nanostructures [1] by glancing angle

deposition of gold films followed by thermal annealing. In addition, we have used three-dimensional kinetic lattice Monte Carlo (KLMC) simulations [2] to understand the structural evolution of the glancing angle deposited Au films on silica templates.

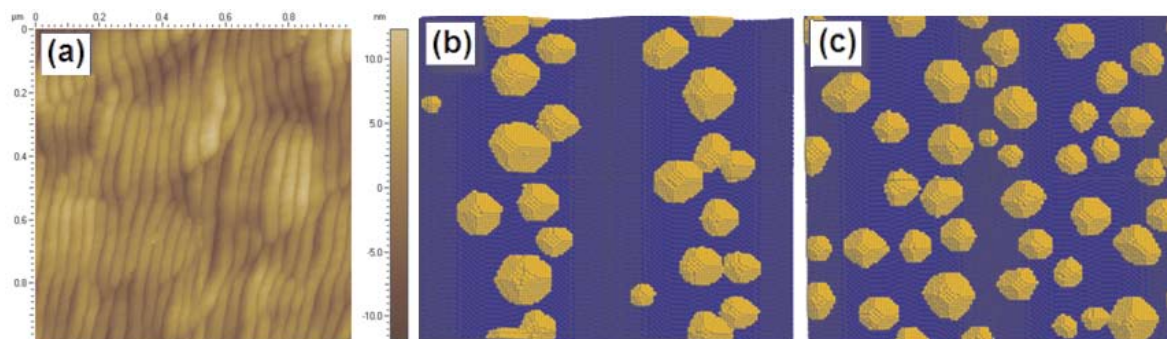


Fig. 1. (a) Atomic force microscopy (AFM) image of ripples created by fluence of 7×10^{17} ions/cm². The wavelength and amplitude of ripples are about 35 nm and 1.5 nm respectively. Images from our atomistic simulations after annealing of 1nm (nominal thickness) gold film of depositions (b) perpendicular to ripple directions, and (c) parallel to ripple direction. The results are from the simulations of 26nm×26nm area of the silica substrate with artificially created ripples of wavelength of 17nm and amplitude of 3 nm. Angle of incidence in these simulations was 45°. Gold nanostructures are depicted in yellow while silica substrate is represented with blue color.

The glancing angle depositions produce inhomogeneity in the film thickness which results in preferential dewetting at thinnest regions on annealing [1]. Our KLMC results show that the deposition of the films at glancing angle perpendicular to ripples, upon annealing, induces the formation of gold nanoparticles aligned along the ripple ridges (Fig. 1(b)). However, in case of depositions at glancing angles parallel to ripples with subsequent annealing results into more homogeneous distribution of nanoparticles on the surface (Fig. 1(c)).

REFERENCES

- [1] T. W. H. Oates, A. Keller, S. Noda and S. Facsko, Appl. Phys. Lett. 93 (2008) 063106.
- [2] M. Strobel, K.-H. Heinig, W. Möller, A. Meldrum, D.S. Zhou, C.W. White, R.A. Zuhr, Nucl. Instr. and Meth. Phys. Res., Sect. B 147 (1999) 343.

4.5 RADIATION BIOLOGY

4.5.1 Status of the Radiation Biology Beam line

A. Sarma, P. Barua, A. Kothari, E.T. Subramaniam, M. Archunan

The specially designed beam line can deliver beams of proton, ⁷Li, ¹¹B, ¹²C, ¹⁴N and ¹⁶O. The flux can be controlled from 10² particles/sec/cm² to 10⁶ particles/sec/cm². The exit

window is having 40 mm diameter with active area for cell irradiation defined by the standard 35 mm petri-dish are. The uniformity is about 95% over 35 mm diameter. The flux control is done by adjusting a double slit through CAMAC from control room. A pre-set controller for faraday cup ensures the exposure repetition as per user requirement.

The Automatic Sample Irradiation system for Radiation Biology Experiment, Aspire, has been installed and being used by the user community. This system takes care of the remote handling of petri dishes in an enclosed sanitised environment during irradiation, multiple irradiations of one sample after another without losing time and keeping the petri-dishes in the medium when they are not being irradiated. The system is controlled by a Linux based software. Further works are going on towards more efficient electronics for dosimetry.



Fig.1. Multi axis positioning system Aspire in the beam line

4.5.2 Status of the Molecular Radiation Biology Laboratory

A. Sarma

The laboratory is designed to extend user support to the best possible way during experiments. The experiments that are undertaken recently require suitable inhouse facilities for relevant protocols. The laboratory facility includes autoclave, biosafety cabinet, two CO₂ incubators, and other normal equipment like microbalance, oven, refrigerated centrifuge, PCR machine, Gel Doc, FIGE system and Semi dry transblotter, -80 C Ultra Freezer [Heto] and a -20 C Deep Freezer [Vest Frost]. and a large capacity 4 C freezer.

In addition we also have a fluorescent microscope [Carl Zeiss] to facilitate the experiments based on FISH and immunofluorescent assays.

For accurate cell counting, a Coulter Cell Counter [Beckman Coulter] is installed in the laboratory. This equipment would drastically enhance the speed and accuracy of post irradiation cell plating during the beam time, and thus save a lot of time. In addition we also have procured an image based cell viability measurement system Countess from Invitrogen.

Initial works with HeLa cells have been started and in order to provide exposure to research scholars to real life experiments, initial cell survival studies using gamma ray and C and O beam has been carried out. In addition to that preparation of cDNA for studying gene expression and the microscopic evaluation of apoptosis using fluorescent dye like Hoechst 33258 has also been carried out. The cell culture works with breast cancer cell line CHAGO has also been started.

Some works have been initiated to study the interaction of gold nano particles with HeLa cells using SEM and Surface Enhanced Raman spectroscopy.

4.6 ATOMIC PHYSICS

T. Nandi

Atomic Physics research facilities with Pelletron accelerator are done in general purpose scattering chamber (GPSC) and in a dedicated beam line in beam hall II. One Doppler tuned spectrometer was developed in GPSC in 2007. This year we have made another ready for high resolution x-ray spectroscopy experiments. A thorough test run will be taken next year. In the mean time some progress has been made on the experimental facilities in beam hall II and some details are given below.

4.6.1 A set up for studying the role of hyperfine splitting on inner shell ionization phenomenon

T. Nandi, B. P. Mohanty, Mumtaz Oswal. S.K. Saini, A. Kothari and P. Barua

Dedicated atomic physics beam line has been shifted into the beam hall-II from beam hall I. Some new features have been added as shown in a schematic (Figure 1). It includes a versatile setup for charge state fraction measurements of post-collisional projectile ions. This setup can also be used for inner shell ionization cross section measurements and beam foil spectroscopy. Beam line includes a retractable Faraday cage, a gate valve, two beam collimating slit systems, an inclined straight electrostatic analyzer (ISESA), a trapper drift tube chamber, 2 movable Faraday cups and a Position Sensitive Proportional Counter (PSPC).

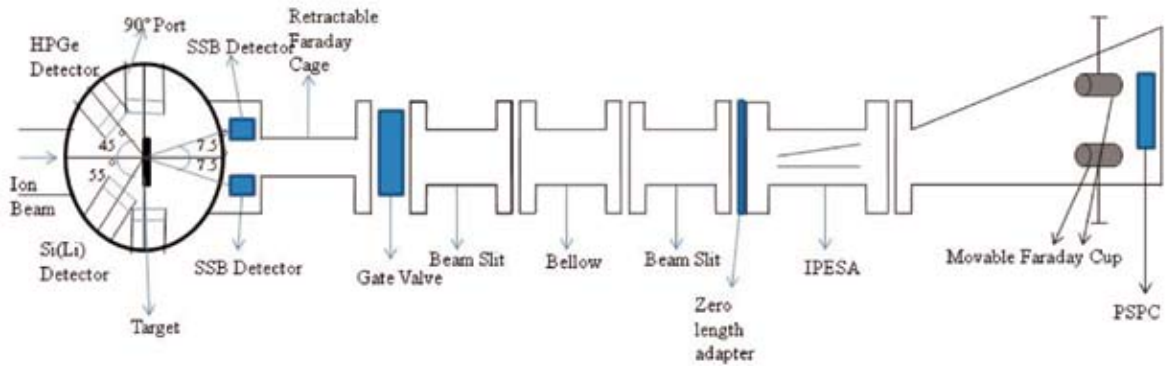


Fig. 1. Experimental set up of Atomic Physics Beam Line

Target chamber is modified to have both types of targets solid as well as gas targets. For gas targets a gas cell with a gas handling system have been fabricated at our work shop to use any one gas bottles out of three gas bottles for natural Xe, ^{131}Xe and ^{132}Xe at a time. Retractable Faraday cage will allow one to check the beam line alignment whenever necessary. Trapper drift tube is 1.5 m long and will be used for charge state fraction measurements experiments. Two movable Faraday cups in trapper drift tube are planned to handle high beam current during the measurement of x-ray and projectile ions in coincidence. For example, unchanged projectile ions can be dumped in a Faraday cup and electron captured projectile ions go to the PSPC when an electric field is applied in IPESA and other one is kept fixed to check the beam alignment at any time by switching off the electric field to the IPESA.

Beam line up to target chamber has been tested using the solid as well gas targets to study the effect of hyperfine splitting on inner shell ionization cross section. Preliminary results obtained are reported in section 5.4.1. Test run of the whole setup by including the charge state fraction setup will be done in next year.